Wind-Aware Trajectory Planning for Fixed-Wing Aircraft in Loss of Thrust Emergencies.

Saswata Paul*, Frederick Hole†, Alexandra Zytek* and Carlos A. Varela*
Department of Computer Science*; Department of Mechanical, Aerospace, and Nuclear Engineering†
Rensselaer Polytechnic Institute, Troy, New York, 12180
{pauls4, holef, zyteka}@rpi.edu, cvarela@cs.rpi.edu

***Abstract*—Loss of thrust (LOT) emergencies create the need for quickly providing pilots with valid trajectories for safely landing the aircraft. It is easy to pre-compute total lost of thrust trajectories for every possible initial point in a 3D flight plan, but it is impossible to predict variables like the availability of partial power, wing surface damage, and wind aloft in advance. Availability of partial power can affect the glide ratio of an aircraft while the presence of wind can significantly affect the trajectory of a gliding aircraft with respect to the ground, e.g. – a tailwind or a headwind can aid or hinder straight line glide by increasing or decreasing the ground speed. Wind can also change the shape of turns from circular to trochoidal, moving an aircraft away from its intended position. In this paper, we present a robust trajectory generation system that can take these dynamic factors into consideration. Our approach outputs valid trajectories to a target runway in the presence of constant, horizontal wind, by using purely geometric criteria for computing flyable trajectories. We model the effect of wind on different components of a possible trajectory by taking into account the observed glide ratio of the aircraft (computed from actual flight performance data) and the horizontal wind vector. We also take into account the effect of wind on ground-speed, the effective glide ratio with respect to the ground, and the shape of turns to calculate trajectories to a virtual point in 3D space which can lead an aircraft to an actual target runway. We introduce an analytical approach for calculating the virtual point for trajectories with left-straight-left or right-straight-right Dubins path segments and a heuristic iterative approach for other cases. Our approach generates trajectories that can lead an aircraft from an initial configuration (latitude, longitude, altitude, heading) to a target configuration in the presence of a constant horizontal wind. In our experiments, the computation time for trajectories ranged from 40 milliseconds to 60 milliseconds.**

I. Introduction

Aircraft loss of thrust emergencies may be caused by various factors, e.g. – fuel exhaustion and bird strike in the cases of Tuninter Flight-1153 [1] and US Airways Flight-1549 [2] incidents respectively. In such situations, the response time is critical and it becomes necessary to provide pilots with feasible trajectories to nearby runways as quickly as possible. A feasible trajectory is one which the aircraft is capable of following under the emergency conditions. It is not possible to anticipate dynamic factors such as the availability of partial power, wing-surface damage, and wind aloft, all of which need to be taken into consideration for computing accurate and valid trajectories in case of a LOT emergency. Dynamic Data-Driven Applications and Systems (DDDAS), used in prediction-based applications, use sensor data to dynamically update a system's model in order to improve the accuracy and effectiveness of the model [3]. In [4], we have investigated Dynamic Data-Driven Avionics Software in decision support systems for LOT emergency scenarios. We presented a system for generating feasible trajectories for LOT scenarios by distilling a complex aerodynamic model to two variables: *glide ratio* and *radius of turn* for discrete bank angles and drag configurations. Our model predicts different glide ratios and different radii of turns by using the aircraft's *baseline glide ratio* – the glide ratio for a clean configuration assuming best gliding airspeed in straight flight. However, the algorithm does not take into account the effect of wind while generating trajectories to target runways.

Wind has a profound effect on the shape of trajectories flown with respect to the ground, leading to significant changes in the shape and position of the resulting ground projections. Wind also affects ground-speed in a non-linear way, thus impacting the overall gliding range of an aircraft. Owing to these factors, in the presence of wind, both the horizontal and vertical profiles of a trajectory, that is valid under no-wind conditions, are significantly altered, enough to potentially render the trajectory infeasible. Therefore, it calls for the need of an inclusive system that can compute accurate trajectories by taking into account both the observed baseline glide ratio (g_0) of an aircraft and the *horizontal wind vector* ($\overrightarrow{w}$). In this paper, we complement our preliminary work by presenting an approach for modeling the effect of wind on the different types of trajectories defined in [4]. This wind model is then used by our dynamic data-driven system to predict the effect of wind and generate trajectories that are feasible in the presence of wind.

We define an *air trajectory* to be a three-dimensional path with respect to the moving airmass while its corresponding *ground trajectory* is the three-dimensional projection with respect to the ground frame of reference. A *no-wind air trajectory* to a target runway is not corrected for wind and might take an aircraft away from the runway. Our approach generates a *wind-aware air trajectory* to a *virtual runway* – a point that lies on the wind vector passing through the actual target runway. The ground trajectory of this wind-aware air trajectory can successfully bring an aircraft down to the target runway, assuming that the aircraft always maintains the

best gliding airspeed. We present an analytical approach for computing the required position of the virtual runway and a heuristic iterative approach for cases which are not considered by our analytical approach. We make decision making easy for the pilots by providing them with trajectories that consist of a series of standard maneuvers (constant-bank turns and straight line gliding segments).

The rest of the paper is divided as follows: Section II discusses prior work on avionics systems and related work on flight path planning in the presence of wind, Section III describes the aircraft aerodynamic model used in our work, Section IV describes how the effect of horizontal wind on a three-dimensional trajectory can be modeled, Section V describes the strategy for generating wind-aware air trajectories proposed in this paper, Section VI describes the details of the experiments performed and Section VII discusses conclusions and possible directions of future work.

II. Related Work

Dubins curves [5] are used for generating two-dimensional trajectories for vehicles with a bounded turning radius. The problem of computing optimal paths in the presence of a constant wind using Dubins paths has previously been investigated. McGee *et al.* [6] explored a method for computing shortest paths by formulating an optimization problem to find the optimal path in a two-dimensional plane. Techy *et al.* [7] described a framework for minimum-time path planning in which they characterize paths in the ground frame of reference by using kinematic equations in the trochoidal frame and derive a condition for optimality. Both of these approaches refined the problem of finding a valid trajectory in the presence of wind to that of intercepting a target (the virtual runway) moving away from the actual runway in the upwind direction. However, their work was focused on trajectory planning in the two-dimensional horizontal plane for aircraft flying at a constant altitude and did not take into account the change in altitude of the aircraft or its flight capabilities.

Dubins curves have also been implemented for computing three-dimensional aircraft paths. Atkins *et al* [8], [9] defined emergency trajectories which had intermediate 'S' turns to lose excess altitude that might take an aircraft too far away from the runway. Owen *et al* [10] proposed trajectories for UAVs with power for maneuverability and introduced intermediate arcs for losing altitude. In [4] we presented an algorithm based on a dynamic data-driven approach for generating trajectories in LOT emergencies by computing a value of the baseline glide ratio from aircraft sensor data. Our trajectories removed the need for 'S' turns and intermediate arcs, thus minimizing the variety of maneuvers in a trajectory. We also ranked the trajectories by a utility function based on certain safety metrics. Nevertheless, previous work on three-dimensional trajectory generation did not consider the effect of wind on trajectories during the generation phase.

In this paper, we improve upon previous work by introducing a new wind modeling paradigm that takes into account the real-time wind conditions and the observed baseline glide ratio of an aircraft in the event of a LOT emergency. This wind model allows our dynamic data-driven system to predict the effect of horizontal wind on a no-wind air trajectory. This prediction is then used for generating an accurate wind-aware air trajectory to a virtual runway.

Our prior work on data streaming application for avionics systems include PILOTS – a ProgrammIng Language for spatiO-Temporal data Streaming applications which can detect sensor failures from data and estimate quantities of interest like aircraft airspeed and fuel quantity upon fault detection and isolation [11], development of failure models to detect errors in aircraft sensor data [12], simulation of error detection and correction using real data from flights [13], development of error signatures to detect abnormal conditions from aircraft sensor data and classify them [14], developing formal definition of error signatures and error recovery from sensor data [15] and programming model to reason about spatio-temporal data streams [16]. We have also successfully implemented PILOTS using data from real-life incidents, as in the case of Tuninter 1153, where a wrong fuel quantity indicator resulted in fuel exhaustion and engine failure [17].

III. Aircraft Model

Stengel [18] defines the position of a point with respect to a three-dimensional inertial frame as:

$$[x\ y\ z]^\top$$

Therefore, the velocity (v) and linear momentum (p) of a particle are given by:

$$v = \frac{\mathrm{d}\,[x\ y\ z]^\top}{\mathrm{d}t} = [\dot{x}\ \dot{y}\ \dot{z}]^\top = [v_x\ v_y\ v_z]^\top$$

$$p = mv = m\,[v_x\ v_y\ v_z]^\top$$

where m = mass of the particle. Fig 1b shows the inertial velocity of a point mass in polar coordinates, where γ is the vertical flight path angle and λ is the horizontal flight path angle. Considering the motion to be a straight line motion in a particular direction, we can use v_x to denote motion in the xy horizontal plane. Two dimensional equations for motion of a point mass, which coincides with the center of mass of an aircraft, restricted to the vertical plane are given below:

$$[\dot{x}\ \dot{z}\ \dot{v_x}\ \dot{v_z}]^\top = [v_x\ v_z\ f_x/m\ f_z/m]^\top$$

Transforming velocity to polar coordinates:

$$\begin{bmatrix}\dot{x}\\ \dot{z}\end{bmatrix} = \begin{bmatrix}v_x\\ v_z\end{bmatrix} = \begin{bmatrix}v\cos\gamma\\ -v\sin\gamma\end{bmatrix}$$

$$\implies \begin{bmatrix}v\\ \gamma\end{bmatrix} = \begin{bmatrix}\sqrt{v_x^2+v_z^2}\\ -\sin^{-1}(v_z/v)\end{bmatrix}$$

Therefore, rates of change of velocity and flight path angle are given by:

$$\begin{bmatrix}\dot{v}\\ \dot{\gamma}\end{bmatrix} = \begin{bmatrix}\frac{\mathrm{d}}{\mathrm{d}t}\sqrt{v_x^2+v_z^2}\\ -\frac{\mathrm{d}}{\mathrm{d}t}\sin^{-1}(v_z/v)\end{bmatrix}$$

Longitudinal equations of motion for a point mass are given by:

$$\dot{x}(t) = v_x = v(t)\cos\gamma(t) \tag{1}$$

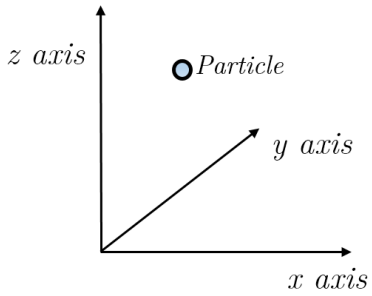

(a) Position of a particle with respect to a 3D inertial frame.

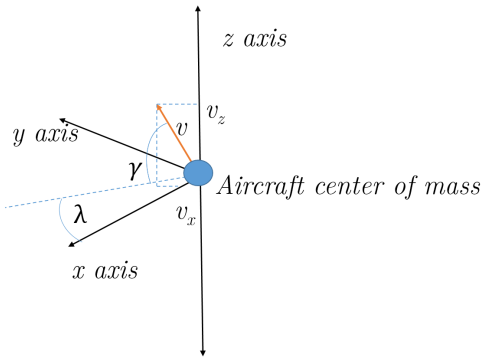

(b) Inertial velocity expressed in polar coordinates.

Fig. 1: Position and inertial velocity of a point mass in a 3D frame.

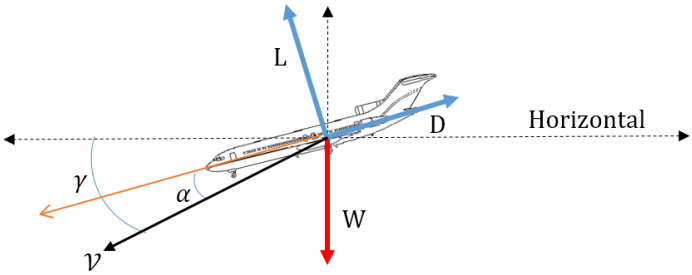

(a) Forces on a gliding flight.

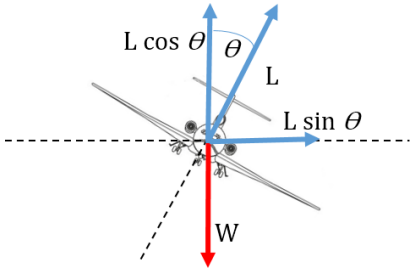

(b) Weight vs lift in banked turns.

Fig. 2: Forces on a glider in straight line motion and banked turns.

$$\dot{z}(t) = v_z = -v(t)\sin\gamma(t) \tag{2}$$

$$\dot{v}(t) = \frac{(C_T\cos\alpha - C_D)\frac{1}{2}\rho(z)v^2(t)S - mG\sin\gamma(t)}{m}$$

$$\dot{\gamma}(t) = \frac{(C_T\sin\alpha + C_L)\frac{1}{2}\rho(z)v^2(t)S - mG\cos\gamma(t)}{mv(t)}$$

where C_T is side force coefficient, C_D is drag coefficient ρ is density of air, α is the angle of attack, C_L is lift coefficient, S is the surface area of the wing and G is the gravitational constant (11.29 kn^{2}ft^{-1}). Lift and Drag are given by $L = C_L\frac{1}{2}\rho v^2 S$, $D = C_D\frac{1}{2}\rho v^2 S$. Thus, for a gliding flight, the condition of equilibrium is defined by the following equations:

$$L = C_L\frac{1}{2}\rho v^2 S = W\cos\gamma$$

$$D = C_D\frac{1}{2}\rho v^2 S = W\sin\gamma$$

where W is the weight of the aircraft.
Therefore, the gliding flight path angle (Fig. 2a) can be found:

$$\cot\gamma = \frac{L}{D} \tag{3}$$

From equations 1 and 2 , we have $\dot{x} = v\cos\gamma$, $\dot{z} = -v\sin\gamma$. Therefore,

$$\cot\gamma = \frac{\dot{x}}{-\dot{z}} = \frac{\Delta x}{-\Delta z} = g_0 \tag{4}$$

where g_0 is the baseline glide ratio. Hence, from equations 3 and 4, we can conclude that $g_0 = \frac{L}{D}$. Therefore, glide range is maximum when (L/D) is maximum. For banked turns, if the bank angle is θ, the vertical component of lift, $L' = L\cos\theta$ (Fig. 2b).

$$g(\theta, k) = \frac{L'}{D} = \left(\frac{L}{D}\right)\cos\theta = g(k)\cos\theta$$

where k is the drag configuration. The drag multiplier function $\delta(k)$ is a ratio that can be used to obtain the baseline glide ratio $g(k)$ for a drag configuration k from the baseline glide ratio of clean configuration g_0.

$$g(k) = g_0\delta(k)$$

Given the baseline glide ratio g_0 and a drag configuration k, the glide ratio for a bank angle θ can be obtained from equation 5.

$$g(\theta, k) = g_0\delta(k)\cos\theta \tag{5}$$

Given the horizontal aircraft airspeed v_x, the radius of turn $r(\theta, v_x)$ for a bank angle θ can be obtained from equation 6.

$$r(\theta, v_x) = \frac{v_x^2}{G\times\tan\theta} \tag{6}$$

Equations 5 and 6, form the basis of our geometrical model of a gliding flight. In the rest of the paper, we will use v to refer to v_x.

IV. Modelling the Effect of Wind on Trajectories

In the case of a LOT emergency, the nature of trajectories depends upon several factors – the baseline glide ratio of the aircraft, the aircraft airspeed, the heading and location of the

emergency, the heading and location of the runway and the wind conditions. In [4], we have defined valid no-wind air trajectories that take into account all of the above factors except for the wind conditions. These no-wind air trajectories consist of three-dimensional Dubins paths followed by spiral maneuvers and extended runway segments. The presence of wind can significantly alter the ground trajectories of these air trajectories. In this section, we model the effect of horizontal wind on an air trajectory.

There are five unique segments of a trajectory as defined in [4] (Fig. 3). They are:

1) Curve 1 of the Dubins path - $\mathcal{C}1$.
2) Straight Line Segment of the Dubins Path - $\mathcal{S}1$.
3) Curve 2 of the Dubins path - $\mathcal{C}2$.
4) Spiral Segment - $\mathcal{C}3$.
5) Extended Runway Segment - $\mathcal{S}2$.

Each of these segments (if present) in a trajectory is affected in a different way. Hence, in order to model the effect of wind on the entire trajectory, we need to model the effect of wind on each segment independently and calculate the amount of shift (ψ) of the endpoint, the time (t) of flight and the total altitude loss (δz) for each of them.

Aircraft paths are composed of two basic movements: banked turns and straight line segments. In the case of banked turns, the original circular arcs are affected by the wind to produce trochoidal tracks above the ground. A trochoid (Fig. 4a) is a geometrical figure that is formed by the locus of a fixed point (x, y) on the circumference of a circle, the centre (c_x, c_y) of which moves along a straight line. The general equations which define a point on a trochoid are:

$$x(t) = c_x(t) + r\cos\phi$$

$$y(t) = c_y(t) + r\sin\phi$$

$$c_x(t) = c_{x_0} + (\mathrm{w}_x \times t)$$

$$c_y(t) = c_{y_0} + (\mathrm{w}_y \times t)$$

where ϕ is the angular distance of the point from the centre, (c_{x_0}, c_{y_0}) is the initial centre and $(\mathrm{w}_x, \mathrm{w}_y)$ are the velocities of the movement of the centre in the two-dimensional plane given the horizontal wind vector $\overrightarrow{\mathrm{w}}(\mathrm{w}, \lambda_{\mathrm{W}})$.

In the case of straight line segments, the aircraft still follows a linear path with respect to the ground, but the actual direction of that line is different from the original intended path (Fig. 4b). The new path can be calculated by calculating the lateral shift (ψ) arising due to the crosswind component of the wind:

$$\psi = \mathrm{w}\sin\alpha \times t$$

where t is the time taken to fly the intended linear path, α is the angle between the heading of the aircraft and the wind direction and $\mathrm{w}\sin\alpha$ is the crosswind component.

Effect of Wind on Turns

Let the initial and final points of the airmass curve $\mathcal{C}$ be $(x_i, y_i, z_i, \lambda_i)$ and $(x_f, y_f, z_f, \lambda_f)$ respectively where $x,\ y,\ z$ and λ represent the latitude, longitude, altitude and heading of the aircraft at a point. If the radius of turn is r (Eq. 6), then the inscribed angle of $\mathcal{C}$ is given by:

$$\Delta\phi = \cos^{-1}\left(1 - \frac{(x_i - x_f)^2 + (y_i - y_f)^2}{2 \times r^2}\right)$$

The time taken $t_{\mathcal{C}}$ can now be derived as:

$$t_{\mathcal{C}} = \frac{\Delta\phi \times r}{v}$$

where v is the aircraft airspeed. Therefore, the total shift of the centre of rotation for $\widehat{\mathcal{C}}$, which is the ground trajectory of $\mathcal{C}$, is given by:

$$\psi_{\mathcal{C}} = t_{\mathcal{C}} \times \mathrm{w}$$

Now, the *effective glide ratio* ($g_e(t)$) throughout $\widehat{\mathcal{C}}$ is given by:

$$g_e(t) = g_0 \times \cos\theta \times \frac{(v_g)}{v} \tag{7}$$

where $v_g(t)$ is the ground-speed given by:

$$v_g(t) = v + (\mathrm{w} \times \cos\alpha(t))$$

where $\alpha(t) = (\lambda_v(t) - \lambda_{\mathrm{W}})$ and $\lambda_v(t)$ is the direction of the aircraft airspeed which varies with time in a turn.

Therefore, the total loss in altitude $(\delta z)_{\widehat{\mathcal{C}}}$ in $\widehat{\mathcal{C}}$ is given by:

$$(\delta z)_{\widehat{\mathcal{C}}} = z_i - z_f$$

The above model applies to parts $\mathcal{C}1$, $\mathcal{C}2$ and $\mathcal{C}3$ of a trajectory which are all constant-bank turns.

Effect of Wind on Straight Line Segments

Let the initial and final points of a straight line part of the no-wind trajectory be $A = (x_A, y_A, z_A, \lambda_A)$ and $B = (x_B, y_B, z_B, \lambda_A)$ respectively (Fig. 4b). Therefore, the original straight line part of the no-wind air trajectory is $\overrightarrow{AB}$, represented by $\mathcal{S}$. Now, let the final point of the straight line part in the corresponding ground trajectory $\widehat{\mathcal{S}}$ be $C = (x_C, y_C, z_C, \lambda_A)$. Time ($t_{\mathcal{S}}$) required to cover distance $\overrightarrow{AB}$ is given by:

$$t_{\mathcal{S}} = \frac{|\overrightarrow{AB}|}{v}$$

We know that the heading of aircraft airspeed throughout $\overrightarrow{AC}$ is λ_A. Therefore, the ground-speed throughout the $\overrightarrow{AC}$ is given by:

$$v_g = v + \mathrm{w} \times \cos\alpha$$

where $\alpha = \lambda_A - \lambda_{\mathrm{W}}$.
Therefore, the new distance $|\overrightarrow{AC}| = t_{\mathcal{S}} * v_g$. Let the angle between $\overrightarrow{AB}$ and $\overrightarrow{AC}$ be Θ.

$$\Theta = \tan^{-1}\frac{\mathrm{w} \times \sin\alpha}{v}$$

The shift $|\overrightarrow{BC}|$ is given by:

$$|\overrightarrow{BC}| = t_{\mathcal{S}} \times \mathrm{w} \times \sin\alpha = \psi_{\mathcal{S}}$$

The total loss in altitude is given by:

$$\delta z_{\widehat{\mathcal{S}}} = z_A - z_C = z_A - \frac{|\overrightarrow{AC}|}{g_e}$$

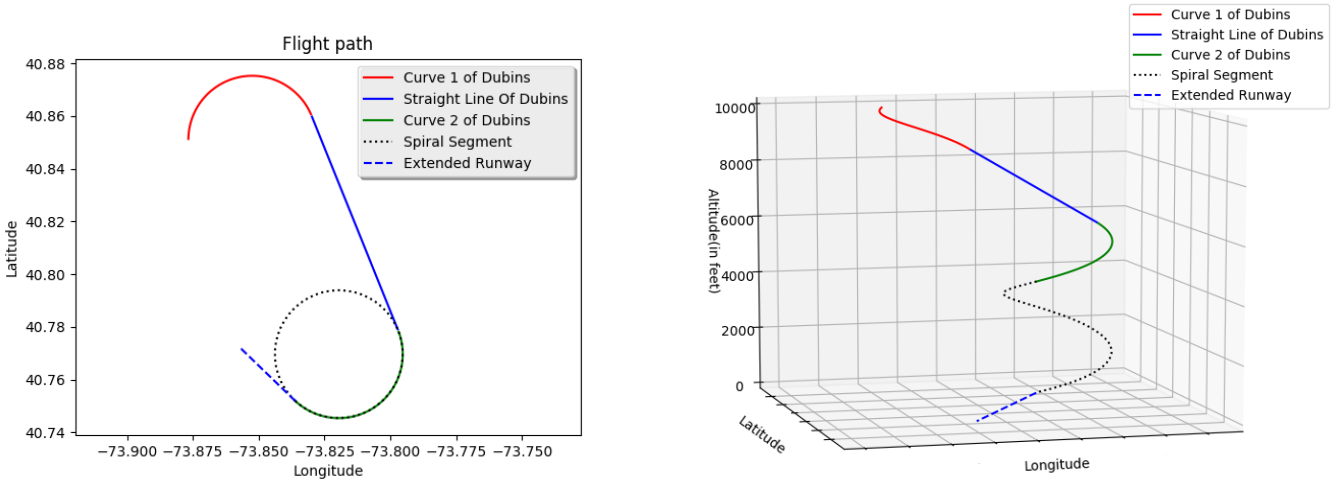

(a) 2D view of a typical trajectory.

(b) 3D view of a typical trajectory.

Fig. 3: Parts of a trajectory.

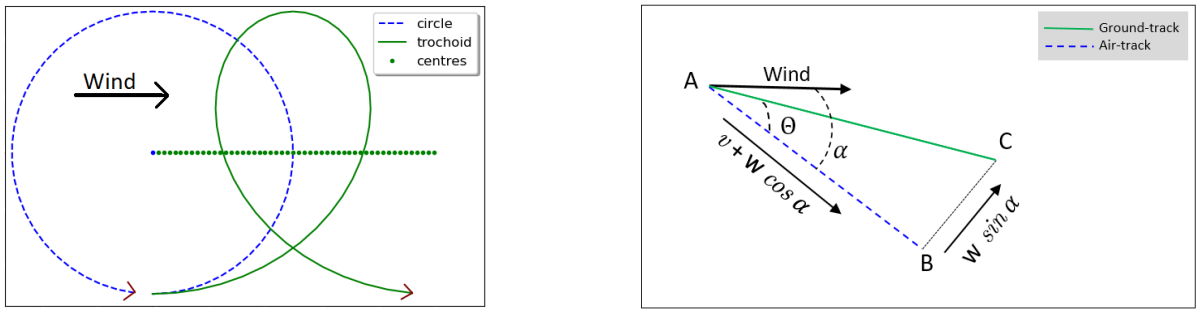

(a) Effect of wind on turns.

(b) Effect of wind on straight line glide.

Fig. 4: Effect of wind on turns and straight line glide.

where g_e is the effective glide ratio in the straight line segment given by:

$$g_e = g_0 \times \frac{v_g}{v} \tag{8}$$

The above model applies to parts $\mathcal{S}1$ and $\mathcal{S}2$ of a trajectory as both represent straight line gliding.

V. Wind-Aware Trajectory Generation

When an aircraft follows a no-wind air trajectory with respect to the airmass, in the presence of wind, the resultant ground trajectory is significantly different. For a wind-aware trajectory to be able to successfully lead a gliding aircraft to a target runway, two conditions have to be met:

- Condition I: *The trajectory must be able to bring the aircraft down to the altitude of the runway.*

  In order for the ground trajectory of a no-wind air trajectory to bring the aircraft down to the required altitude, the total loss in altitude should be equal to the difference between the altitude of the initial position of the aircraft and the altitude of the target runway.

$$(\delta z)_{\mathcal{C}1} + (\delta z)_{\mathcal{S}1} + (\delta z)_{\mathcal{C}2} + (\delta z)_{\mathcal{C}3} + (\delta z)_{\mathcal{S}2} = \Delta z$$

where Δz is the altitude difference between the initial configuration of the aircraft and the target runway.

- Condition II: *The end of the trajectory must meet the coordinates of the runway in the two-dimensional space.*

  In the presence of wind, the ground trajectory of a no-wind air trajectory changes significantly as described in the previous section. It has been previously demonstrated in [6] that in the presence of a constant horizontal wind, the final position of the ground trajectory lies on a line which is parallel to the wind vector and passes through the endpoint of the no-wind air trajectory. Therefore, the problem of finding a wind-aware air trajectory is distilled to the problem of intercepting a virtual target moving away from the actual runway in the upwind direction.

  Therefore, if T is the total time of flight for the original no-wind trajectory, for the wind augmented trajectory to intercept the runway, the following condition must be met:

$$\psi_{\mathcal{C}1} + \psi_{\mathcal{S}1} + \psi_{\mathcal{C}2} + \psi_{\mathcal{C}3} + \psi_{\mathcal{S}2} = T \times \mathrm{w}$$

Now, we know that,

$$T = t_{\mathcal{C}1} + t_{\mathcal{S}1} + t_{\mathcal{C}2} + t_{\mathcal{C}3} + t_{\mathcal{S}2}$$

Therefore,

$$(t_{\mathcal{C}1} + t_{\mathcal{S}1} + t_{\mathcal{C}2} + t_{\mathcal{C}3} + t_{\mathcal{S}2}) \times \mathrm{w} = \psi_{\mathcal{C}1} + \psi_{\mathcal{S}1} + \psi_{\mathcal{C}2} + \psi_{\mathcal{C}3} + \psi_{\mathcal{S}2} \quad (9)$$

In the presence of wind, the effective glide ratio of a gliding aircraft is different from the aerodynamic glide ratio (Eq. 7, Eq. 8), but the *rate of descent* (σ) remains unaffected by horizontal wind (Fig. 5b). Therefore, if an aircraft glides with the best gliding airspeed for time t, then the loss of altitude will always be equal to σt, even though the horizontal distance covered will be different in case of tailwind, headwind, and no - wind conditions.

$$\Delta z(t) = \sigma t \quad (10)$$

Therefore, in order to compute valid wind-aware air trajectories, we make the following assumptions:

1) The aircraft always flies with the best gliding airspeed v.
2) For each segment in an air trajectory, time t is required to fly that segment with respect to the airmass.
3) The aircraft follows each segment of the air trajectory for time t.

Assumptions 1, 2 and 3 imply that a ground trajectory will lose exactly the same amount of altitude as the corresponding air trajectory since the time in air is equal for both. This ensures that Condition I holds. Therefore, the problem of generating a wind-aware air trajectory is reduced to the problem of generating a no-wind air trajectory, the ground trajectory of which can bring an aircraft to the correct position in the horizontal plane: $R = (x, y, \lambda)$. This can be achieved by generating a wind-aware air trajectory to a virtual runway $R' = (x', y', \lambda' = \lambda)$ in the horizontal plane such that Condition II (Eq. 9) is met.

Analytical Solution for Finding R'

For being able to analytically compute the location of the virtual runway, we need to be able to predict the total shift caused by the various segments of the trajectory. In order to simplify the task of prediction, we first generate an initial no-wind air trajectory (P) to the actual runway to model the effect of wind on it and then compute a new wind-aware air trajectory to a virtual runway that has the same type of initial Dubins path, the same integral number of spirals, and an extended runway segment that has the same length and orientation with respect to the wind vector. This allows us to compute $\psi_{\mathcal{C}1}$, $\psi_{\mathcal{C}2}$, $\psi_{\mathcal{C}3}$, $\psi_{\mathcal{S}1}$, and $\psi_{\mathcal{S}2}$ for P and argue that for the new wind-aware air trajectory P', $\psi_{\mathcal{C}3'}$ and $\psi_{\mathcal{S}2'}$ will have the same value as that of $\psi_{\mathcal{C}3}$ and $\psi_{\mathcal{S}2}$ respectively. This is because the same integral number of spirals will always produce the same amount of shift in the presence of a constant horizontal wind, irrespective of their position and two extended runway segments of equal length and orientation with respect to the wind vector will also produce the same shift.

The total shift $\Psi(P')$ caused by the effect of wind on P' is given by:

$$\Psi(P') = \psi_{\mathcal{C}1'} + \psi_{\mathcal{C}2'} + \psi_{\mathcal{S}1'} + \psi_{\mathcal{C}3'} + \psi_{\mathcal{S}2'}$$

For a trajectory in the horizontal plane to be valid, it must satisfy the following constraint, which follows directly from Condition II:

$$\Psi(P') = |\overline{RR'}|$$

Since P and P' have similar $\mathcal{C}3$ and $\mathcal{S}2$, the end point of $\mathcal{C}2'$ should lie on a line passing through the end point of $\mathcal{C}2$ in the upwind direction. Hence, a valid P' satisfies the following condition:

$$\Psi(P') - (\psi_{\mathcal{C}3'} + \psi_{\mathcal{S}2'}) = \psi_{\mathcal{C}1'} + \psi_{\mathcal{C}2'} + \psi_{\mathcal{S}1'} = |\overline{ee'}| \quad (11)$$

where e and e' are the end points of $\mathcal{C}2$ and $\mathcal{C}2'$.

For trajectories whose initial Dubins paths are of the form *left - straight - left* or *right - straight - right*, the total heading change and thus the total curve length of $\mathcal{C}1$ and $\mathcal{C}2$ is the same for all variations of trajectories given that the aforementioned constraints are satisfied. Hence we can conclude that:

$$\psi_{\mathcal{C}1'} + \psi_{\mathcal{C}2'} = \psi_{\mathcal{C}1} + \psi_{\mathcal{C}2} \quad (12)$$

Therefore, from equations 11 and 12, we get

$$|\overline{ee'}| = (\psi_{\mathcal{C}1} + \psi_{\mathcal{C}2}) + \psi_{\mathcal{S}1'} \quad (13)$$

Let the lengths of $\mathcal{S}1$ and $\mathcal{S}1'$ be l and l' respectively and the angle between the heading of $\mathcal{S}1$ and $\overrightarrow{\mathrm{w}}$ be α and the angle between the heading of $\mathcal{S}1'$ and $\overrightarrow{\mathrm{w}}$ be α' (Fig. 6a). Now, time to fly $\mathcal{S}1'$ is given by:

$$t_{\mathcal{S}1'} = \frac{l'}{v + \mathrm{w}\cos\alpha'} \quad (14)$$

and

$$\psi_{\mathcal{S}1'} = t_{\mathcal{S}1'} \times \mathrm{w}\sin\alpha' \quad (15)$$

Since the total heading change and thus the total curve length of $(\mathcal{C}1 + \mathcal{C}2)$ and $(\mathcal{C}1' + \mathcal{C}2')$ are the same, therefore, $(\delta z)_{\mathcal{C}1} + (\delta z)_{\mathcal{C}2} = (\delta z)_{\mathcal{C}1'} + (\delta z)_{\mathcal{C}2'}$. By construction, the total change in altitude for the entire Dubins path segments of P and P' are equal. Therefore,

$$\begin{aligned}(\delta z)_{\mathcal{C}1} + (\delta z)_{\mathcal{C}2} + (\delta z)_{\mathcal{S}1} &= (\delta z)_{\mathcal{C}1'} + (\delta z)_{\mathcal{C}2'} + (\delta z)_{\mathcal{S}1'} \\ \text{or, } (\delta z)_{\mathcal{S}1} &= (\delta z)_{\mathcal{S}1'} \\ \text{or, } \sigma t_{\mathcal{S}1'} &= \sigma t_{\mathcal{S}1} \text{ (from Eq. 10)} \\ \text{or, } t_{\mathcal{S}1'} &= t_{\mathcal{S}1}\end{aligned}$$

From symmetry (Fig. 6a), distance between the end points of $\mathcal{C}2$ and $\mathcal{C}2'$ ($|\overline{ee'}|$) is equal to the distance between their centres ($|\overline{cc'}|$). Hence, from equations 13 and 15, we get:

$$|\overline{cc'}| = \psi_{\mathcal{S}1'} + (\psi_{\mathcal{C}1} + \psi_{\mathcal{C}2}) = (t_{\mathcal{S}1'} \times \mathrm{w}\sin\alpha') + (\psi_{\mathcal{C}1} + \psi_{\mathcal{C}2}) \quad (16)$$

From geometry, we can see that (Fig. 6a),

$$|\overline{cc'}| = k\left(\frac{1}{\tan\alpha} - \frac{1}{\tan\alpha'}\right)$$

where k is the perpendicular distance between the centre of $\mathcal{C}1$ and the line parallel to $\overrightarrow{\mathrm{w}}$ and passing through c. Therefore,

$$(t_{\mathcal{S}1'} \times \mathrm{w}\sin\alpha') + (\psi_{\mathcal{C}1} + \psi_{\mathcal{C}2}) = k\left(\frac{1}{\tan\alpha} - \frac{1}{\tan\alpha'}\right)$$

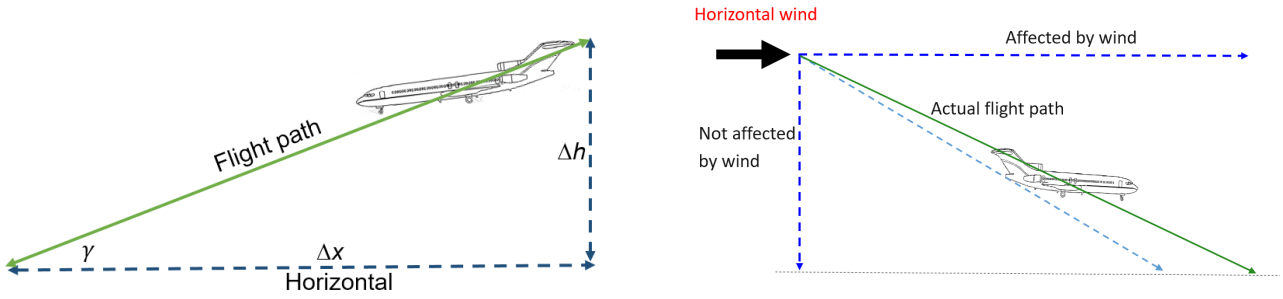

(a) Glide ratio of a gliding aircraft.

(b) Effect of horizontal wind on a gliding aircraft.

Fig. 5: Effect of horizontal wind on glide ratio.

Let $\mathrm{K}_1 = t_{\mathcal{S}1'} \times \mathrm{w}$, $\mathrm{K}_2 = (\psi_{\mathcal{C}1} + \psi_{\mathcal{C}2})$ and $\mathrm{K}_3 = \frac{k}{\tan\alpha} - \mathrm{K}_2$. These are values that can be pre-computed by modeling the effect of wind on P. Therefore, we get:

$$\begin{aligned} \mathrm{K}_1 sin\alpha' + \mathrm{K}_2 &= \frac{k}{\tan\alpha} - \frac{k}{\tan\alpha'} \\ \text{or, } \mathrm{K}_1 sin\alpha' + k\frac{\sin\alpha'}{\cos\alpha'} &= \frac{k}{\tan\alpha} - \mathrm{K}_2 \\ \text{or, } \mathrm{K}_1 sin\alpha' + k\frac{\sin\alpha'}{\cos\alpha'} &= \mathrm{K}_3 \end{aligned}$$

which can be expanded into the following quartic equation in terms of $\sin\alpha'$:

$$\mathrm{K}_1^2 \sin^4\alpha' - 2\mathrm{K}_1\mathrm{K}_3 \sin^3\alpha' + (\mathrm{K}_3^2 + k^2)\sin^2\alpha' - k^2 = 0 \quad (17)$$

From Fig. 6a, we can see that $l' = k/\sin\alpha'$. Therefore, from Eq. 14, we get:

$$\begin{aligned} &\frac{l'}{v + \mathrm{w}\cos\alpha'} = t_{\mathcal{S}1'} \\ \text{or, } &\frac{k}{\sin\alpha'(v + \mathrm{w}\cos\alpha')} = t_{\mathcal{S}1'} \\ \text{or, } &t_{\mathcal{S}1'} \times \sin\alpha'(v + \mathrm{w}\cos\alpha') = k \\ \text{or, } &t_{\mathcal{S}1'} \times v\sin\alpha' + t_{\mathcal{S}1'} \times \mathrm{w}\sin\alpha'\cos\alpha' = k \\ \text{or, } &\mathrm{K}_4 \sin\alpha' + \mathrm{K}_1 \sin\alpha'\cos\alpha' = k \end{aligned}$$

where $\mathrm{K}_4 = t_{\mathcal{S}1'} \times v$. The above equation can be expanded into another quartic equation in $\sin\alpha'$:

$$\mathrm{K}_1^2 \sin^4\alpha' + (\mathrm{K}_4^2 - \mathrm{K}_1^2)\sin^2\alpha' - 2\mathrm{K}_4 k \sin\alpha' + k^2 = 0 \quad (18)$$

Since we have two quartic equations, it now becomes possible to derive the following cubic equation in terms of $\sin\alpha'$ from equations 17 and 18:

$$\begin{aligned} 2\mathrm{K}_1\mathrm{K}_3 \sin^3\alpha' + (\mathrm{K}_4^2 - \mathrm{K}_1^2 - \mathrm{K}_3^2 - k^2)\sin^2\alpha' \\ - 2\mathrm{K}_4 k \sin\alpha' + 2k^2 = 0 \end{aligned} \quad (19)$$

Now, a real value of $\sin\alpha'$ can be computed from Eq. 19 which can be used to calculate $|\overline{cc'}|$ and therefore $|\overline{ee'}|$ using Eq. 16. Finally, we can compute the shift of P' by using Eq. 11, which is the required distance of the virtual target from the actual runway in the upwind direction.

The above approach, however, cannot be implemented for trajectories whose initial Dubins paths are of the type *right - straight - left* or *left - straight - right*. This is because in these types of Dubins paths, the total curve length of $\mathcal{C}1$ and $\mathcal{C}2$ differ for different variations (Fig. 6b). This makes us unable to use $\psi_{\mathcal{C}1} + \psi_{\mathcal{C}2}$ calculated from P as a constant in P'.

Iterative Solution for Finding R'

When the analytical solution for finding R' cannot be applied, we can use a heuristic iterative approach for computing R' as given in Pseudo-code 1.

```
find_virtual_runway(initial_no_wind, runway,
    ↪ wind_heading)
  initial_wind = model_wind(initial_no_wind)
  last_point = final_point(initial_wind)
  deviation = difference(runway, last_point)
  distance = 0
  virtual_point = null
  while(deviation > 0)
    distance = distance + deviation
    reverse_wind_heading = reverse(wind_heading)
    virtual_point = along_heading_at_distance(runway
    ↪ , reverse_wind_heading, distance)
    temp_no_wind = find_no_wind_air_trajectory(
    ↪ virtual_point)
    temp_wind = model_wind(temp_no_wind)
    temp_last_point = final_point(temp_wind)
    deviation = difference(runway, temp_last_point)
  return virtual_point
```

Pseudocode 1: Heuristic iterative approach for computing R'

VI. Experimentation and Results

In our experiments, we generated a no-wind air trajectory from an altitude of 10,000 feet and an initial configuration – {longitude: -73.8767, latitude: 40.8513, heading: 0.698798}, to LGA31 of LaGuardia airport, New York and then implemented our wind model as described in section IV. For the first case, we modeled the effect of a 40 knot wind coming from North, South, East and West (Fig. 7) and for the second case, we modeled the effect of a West-wind of 10, 20, 30 and 40 knots on the same no-wind air trajectory (Fig. 8). We

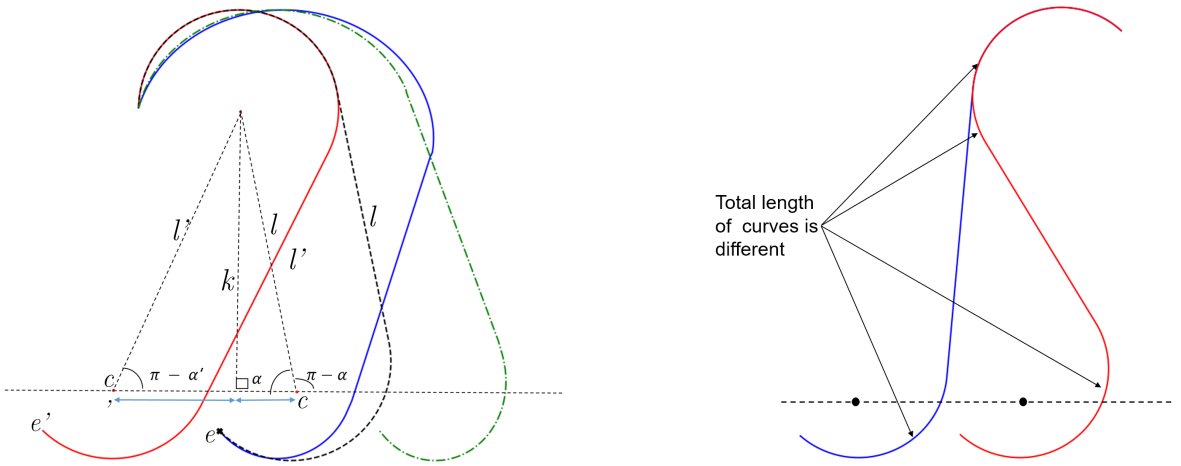

(a) RSR path. (b) LSR path.

Fig. 6: Geometry of RSR (symmetrical to LSL) and LSR (symmetrical to RSL) paths.

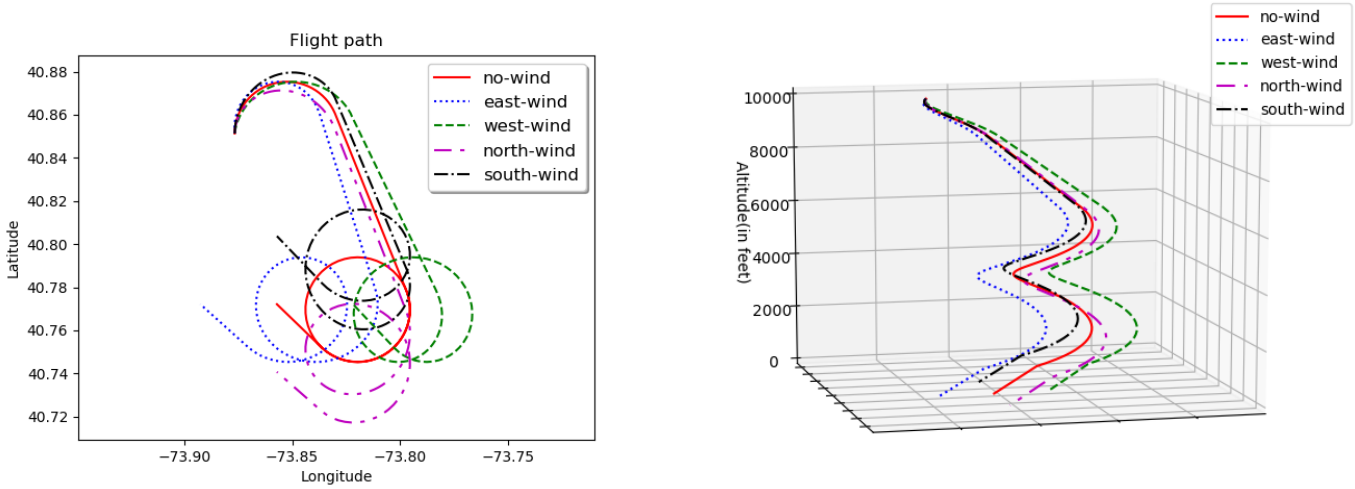

(a) 2D view. (b) 3D view.

Fig. 7: Effect of a 40 knot wind from different directions on a trajectory from 10000 feet.

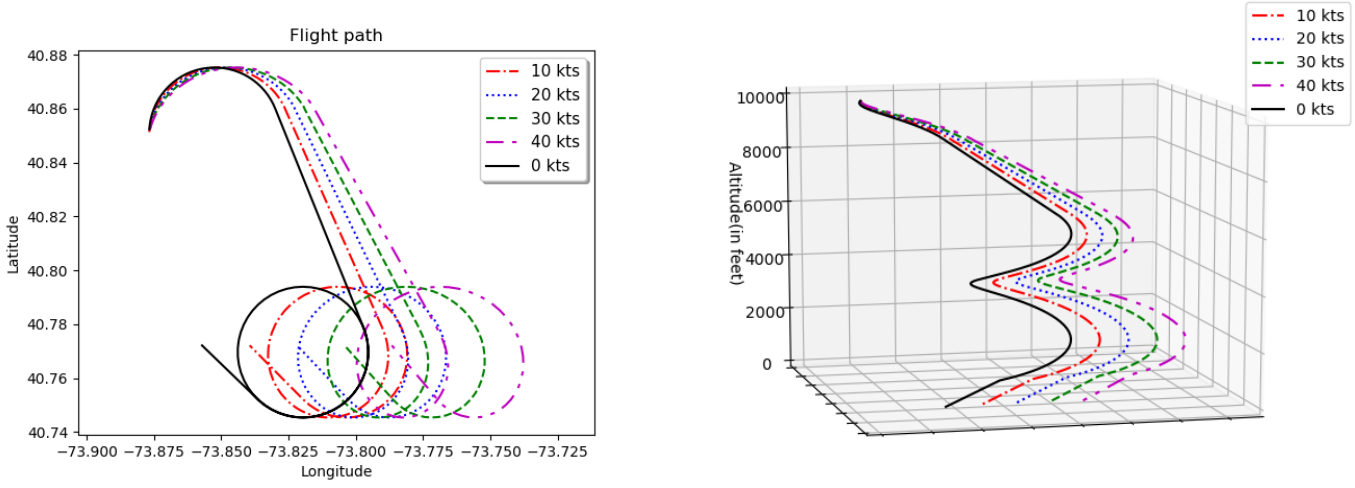

(a) 2D view. (b) 3D view.

Fig. 8: Effect of different magnitudes of West-wind on a trajectory from 10000 feet.

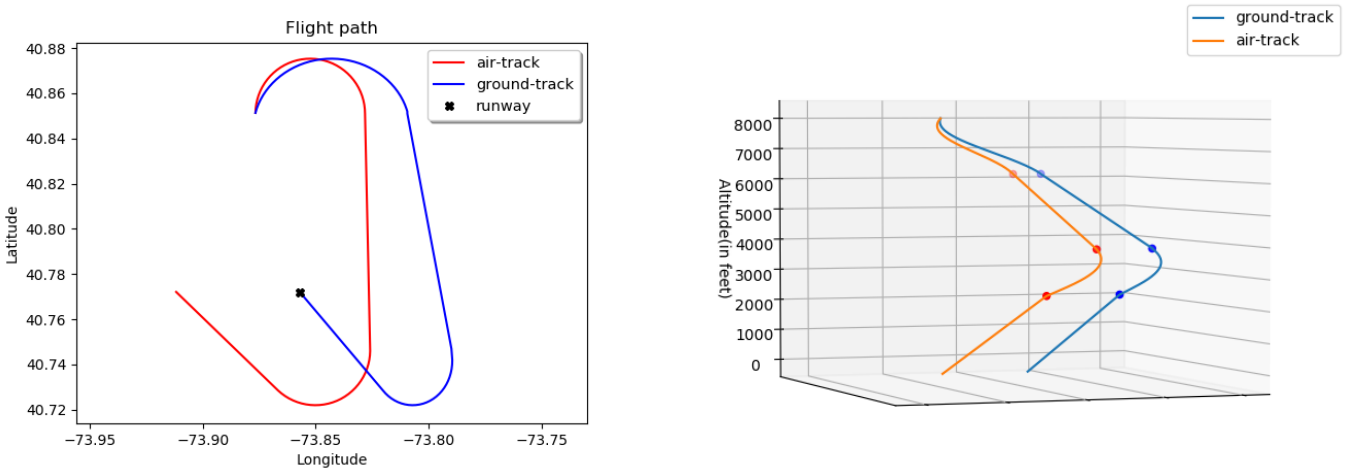

(a) 2D view.

(b) 3D view.

Fig. 9: Wind-aware trajectory from 8000 feet in 40 knots West-wind.

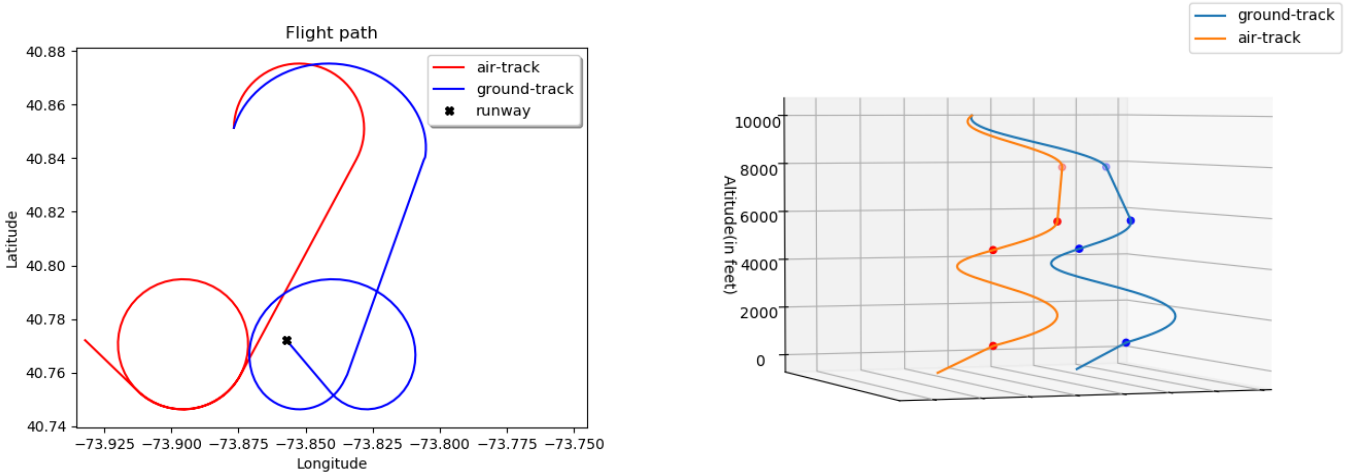

(a) 2D view.

(b) 3D view.

Fig. 10: Wind-aware trajectory from 10000 feet in 40 knots West-wind.

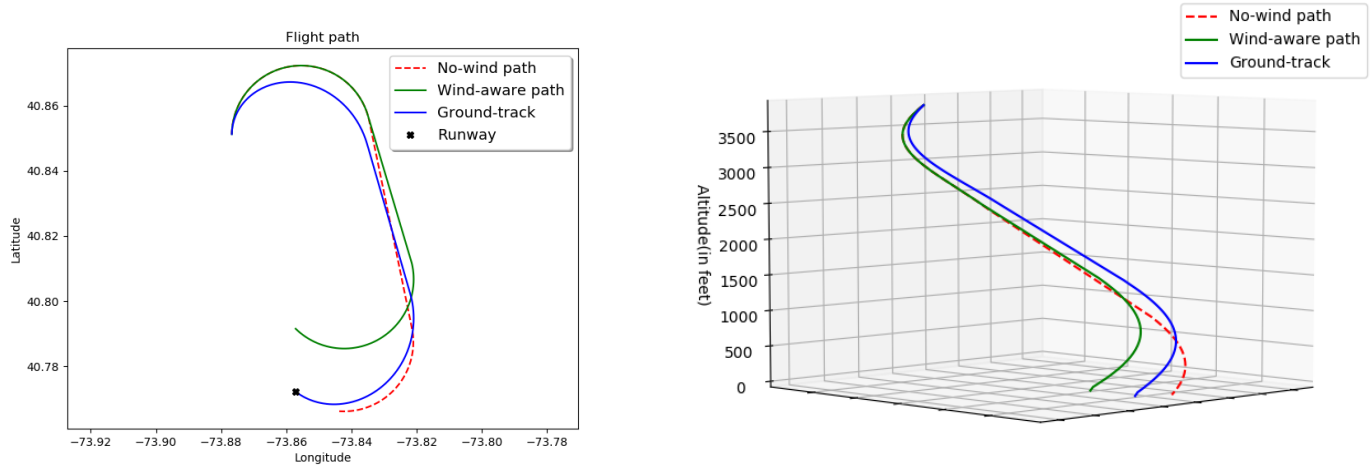

(a) 2D view.

(b) 3D view.

Fig. 11: Wind-aware trajectory to LGA31 from 3850 feet, assisted by a 30 knots North-wind.

also generated wind-aware air trajectories to a virtual runway from altitudes of 8,000 and 10,000 feet in the presence of a 40 knots West-wind (Fig. 9, Fig. 10) that can lead a gliding aircraft to LGA31. We used a clean configuration glide ratio of 17.25:1 for straight line glide as predicted in [19] with a dirty configuration glide ratio of 9:1 for the final extended runway approaches. All our experiments were done for an Airbus A320 using 30° bank angle for the turns. On an average, it took 50 milliseconds to generate results on an Intel Core i7-7500U CPU - 2.70GHz. Using our wind model, we successfully generated a wind-aware trajectory to LGA31 from an altitude of 3850 feet, assisted by a 30 knots North-wind, even though a no-wind trajectory in the same configuration was not possible (Fig. 11). This clearly shows the potential of the model for generating wind-aware trajectories when no-wind trajectories are infeasible.

VII. Conclusion and Future Work

Trajectory generation algorithms which can compute valid trajectories in a short time are crucial during an emergency. Our experiments clearly show that with a proper wind model, it is possible to design prediction based dynamic data-driven systems that can be used to quickly generate wind-aware trajectories in case of LOT emergencies. Trajectories computed using this approach can be guaranteed to be of the highest fidelity since they take into account the capabilities of the aircraft and the wind conditions during an actual emergency. This will allow pilots to quickly decide on a reasonable course of action for safely landing an aircraft without having to manually consider the feasibility of various choices, thus reducing the response time.

Future directions of work include the implementation of variable wind gradients, which is true for real-world scenarios where the wind conditions change with a change in altitude. Designing terrain-aware algorithms that can detect obstacles and generate paths that avoid them is also an interesting direction of work. Traditional obstacle avoidance algorithms depend on graph search techniques which have a high computational time. Therefore, it is necessary to design heuristic obstacle detection algorithms that can produce accurate results in the shortest possible time. Willcox *et al.* [20] compute failure probabilities of maneuvers for aerospace vehicles. Uncertainty quantification is another possible direction of work which will help us to represent conditions such as wind speed, glide ratio, and pilot errors as probability distributions and convert them into a region of possibility around trajectories and allow us to compute the failure probabilities of trajectories.

Acknowledgments

This research is partially supported by the DDDAS program of the Air Force Office of Scientific Research, Grant No. FA9550-15-1-0214 and NSF Grant No. 1462342.

References

[1] ANSV Agenzia Nazionale per la Sicurezza del Volo. "Final Report: Accident involving ATR 72 aircraft, registration marks TL-LBB ditching off the coast of Capo Gallo(Palermo-Sicily)". 2005.

[2] NTSB The National Transportation Safety Board. "Accident Report: Loss of thrust in both engines after encountering a flock of birds and subsequent ditching on the Hudson River US Airways Flight 1549, Airbus A320-214, N106US, Weehawken, New Jersey, January 15, 2009". 2010.

[3] F. Darema. "Dynamic data driven applications systems: New capabilities for application simulations and measurements". In *Computational Science – ICCS 2005*, pages 610–615, Berlin, Heidelberg, 2005. Springer Berlin Heidelberg.

[4] S. Paul, F. Hole, A. Zytek, and C. A. Varela. "Flight trajectory planning for fixed wing aircraft in loss of thrust emergencies". In *Dynamic Data-Driven Application Systems (DDDAS 2017)*, Cambridge, MA, Aug 2017. arXiv:1711.00716 [cs.SY].

[5] L. E. Dubins. "On curves of minimal length with a constraint on average curvature, and with prescribed initial and terminal positions and tangents". *American Journal of Mathematics*, 79(3):497–516, 1957.

[6] T. McGee, S. Spry, and K. Hedrick. "Optimal path planning in a constant wind with a bounded turning rate". In *AIAA Guidance, Navigation, and Control Conference and Exhibit*, page 6186, 2005.

[7] L. Techy and C. A. Woolsey. "Minimum-time path planning for unmanned aerial vehicles in steady uniform winds". *Journal of guidance, control, and dynamics*, 32(6):1736–1746, 2009.

[8] E. M. Atkins, I. A. Portillo, and M. J. Strube. "Emergency flight planning applied to total loss of thrust". *Journal of Aircraft*, 43(4):1205–1216, 2006.

[9] E. M. Atkins. "Emergency landing automation aids: an evaluation inspired by US Airways flight 1549". In *AIAA Infotech@ Aerospace Conference*, Atlanta, Georgia, 2010.

[10] M. Owen, R. W. Beard, and T. W. McLain. "Implementing dubins airplane paths on fixed-wing UAVs". In *Handbook of Unmanned Aerial Vehicles*, pages 1677–1701, Dordrecht, 2015. Springer Netherlands.

[11] S. Imai and C. A. Varela. "A programming model for spatio-temporal data streaming applications". In *Dynamic Data-Driven Application Systems (DDDAS 2012)*, pages 1139–1148, Omaha, Nebraska, June 2012.

[12] S. Imai, S. Chen, W. Zhu, and C. A. Varela. "Dynamic data-driven learning for self-healing avionics". *Cluster Computing*, Nov 2017.

[13] S. Imai, A. Galli, and C. A. Varela. "Dynamic data-driven avionics systems: Inferring failure modes from data streams". In *Dynamic Data-Driven Application Systems (DDDAS 2015)*, Reykjavik, Iceland, June 2015.

[14] S. Imai, R. Klockowski, and C. A. Varela. "Self-healing spatio-temporal data streams using error signatures". In *2nd International Conference on Big Data Science and Engineering (BDSE 2013)*, Sydney, Australia, December 2013.

[15] R. Klockowski, S. Imai, C. Rice, and C. A. Varela. "Autonomous data error detection and recovery in streaming applications". In *Proceedings of the International Conference on Computational Science (ICCS 2013). Dynamic Data-Driven Application Systems (DDDAS 2013) Workshop*, pages 2036–2045, May 2013.

[16] S. Imai and C. A. Varela. "Programming spatio-temporal data streaming applications with high-level specifications". In *3rd ACM SIGSPATIAL International Workshop on Querying and Mining Uncertain Spatio-Temporal Data (QUeST) 2012*, Redondo Beach, California, USA, November 2012.

[17] S. Imai, E. Blasch, A. Galli, W. Zhu, F. Lee, and C. A. Varela. "Airplane flight safety using error-tolerant data stream processing". *IEEE Aerospace and Electronics Systems Magazine*, 32(4):4–17, 2017.

[18] R. F. Stengel. *Flight dynamics*. Princeton University Press, 2015.

[19] K. A. Avrenli and B. J. Dempsey. "Is "Green Dot" always the optimum engines-out glide speed on the Airbus A320 aircraft?". *Journal of Aviation/Aerospace Education & Research*, 24(3):33, 2015.

[20] D. Allaire, J. Chambers, R. Cowlagi, D. Kordonowy, M. Lecerf, L. Mainini, F. Ulker, and K. Willcox. "An offline/online DDDAS capability for self-aware aerospace vehicles". *Procedia Computer Science*, 18:1959–1968, 2013.